MSR-ERO RENDEZVOUS NAVIGATION SENSORS AND IMAGE PROCESSING

Keyvan Kanani[(1)], Alex Marchand[(1)], Alexandre Falcoz[(1)], Christian Kracht[(2)], Tristan Röll[(2)], Thomas Kämpfe[(2)], Antoine Lecocq[(3)], Michaël Richert[(3)], Pierre Goux[(3)], Thierry Bomer[(3)], Léo Novelli[(4)], Leila Lorenzoni[(4)], Manuel Sanchez Gestido[(4)]

(1) Airbus Defence and Space, 31 Rue des Cosmonautes, 31400 Toulouse, France

(2) Jena-Optronik GmbH, Otto-Eppenstein-Straße 3, 07745 Jena, Germany

(3) SODERN 20 Avenue Descartes 94450 Limeil-Brévannes, France

(4) European Space Agency – ESTEC, Noordwijk, The Netherlands

ABSTRACT

In the frame of the ESA/NASA Mars Sample Return (MSR) mission, Airbus Defence and Space, under ESA contract, is designing and developing the Earth Return Orbiter (ERO) spacecraft which aims to capture and to bring back to Earth samples collected on Mars and put into low Mars orbit by NASA. This paper focuses on the vision sensors of MSR-ERO spacecraft used in its closed loop GNC during the rendezvous phase (the last kilometres before capture).

In a first section, the MSR mission is recalled, ERO is presented and the vision sensor trade-off done in the early phases of MSR-ERO project is described. The vision sensors and their associated image processing are then detailed in a second and third sections. The fourth section explains the vision sensor architecture within the ERO system and the sensors operation concept during the in-orbit rendezvous leg of the mission. An overview of their development plans is finally provided in a last section, together with the preliminary performance test results.

1 INTRODUCTION

1.1 The Mars Sample Return mission

The ESA/NASA Mars Sample Return (MSR) campaign aims to return to Earth samples of Mars materials (see [1]). Returning a carefully selected set of samples from Mars to Earth has been a major long-term goal of international planetary exploration for decades. Past Mars missions have confirmed a consensus that finding compelling evidence for past life on Mars requires detailed analysis of a diverse set of carefully selected samples using the full range of the best instruments available on Earth. Beyond the search for life, MSR is expected to help scientists understand the detailed geological history of Mars, the evolution of its climate, and any hazards in the dust of the Red Planet that could affect future human explorers.

NASA's Perseverance Mars rover landed in Jezero Crater in February 2021 and is now collecting and storing a range of compelling samples (see [2]). Under MSR program, NASA will develop a Sample Retrieval Lander (SRL) mission, which would launch in 2028, carrying a rocket known as the Mars Ascent Vehicle (MAV) and an Orbiting Sample (OS) container. The Perseverance rover will deliver to SRL the sample tubes to be assembled in the OS. As a backup, a Sample Recovery Helicopter (SRH) developed by NASA and transported to Mars on the SRL will collect tubes deposited on ground by Perseverance and transport them to SRL. The MAV will then launch from Mars and inject the OS in low Mars orbit. The ESA provided Earth Return Orbiter (ERO) vehicle

will finally autonomously detect and rendezvous with the OS, capture it, seal it, and safely bring it back to Earth in the early 2030s.

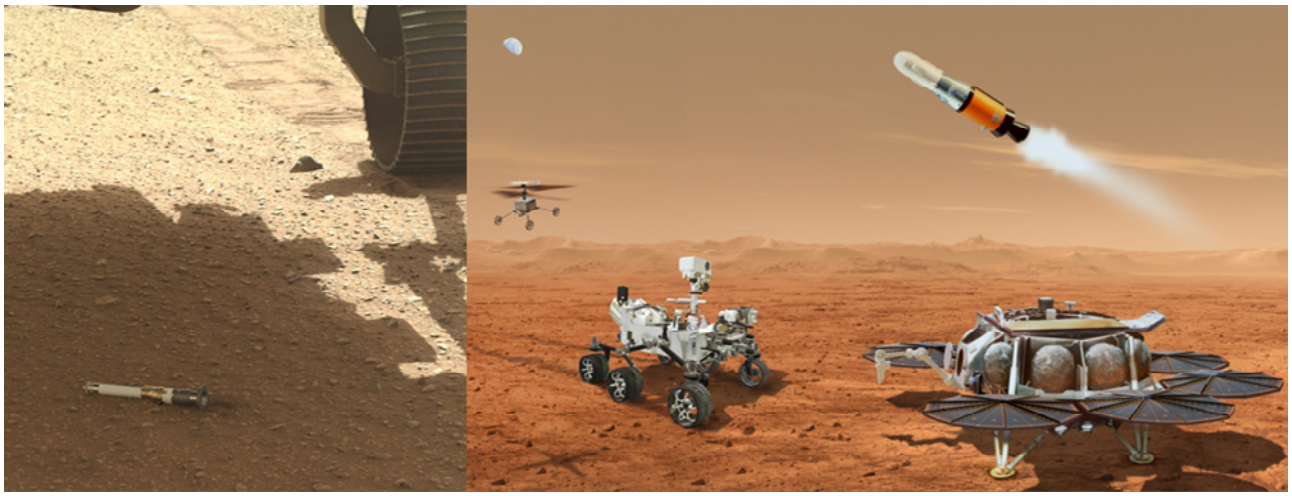

Figure 1. (Left) Sample tube collected by Perseverance and deposited on ground. (Right) Illustration of MSR robotic systems operating on Mars surface (far left: SRH, left: Perseverance, far right: SRL, top right: MAV). Credit: NASA/ESA/JPL-Caltech.

1.2 The Earth Return Orbiter

ERO is a multi-stage modular spacecraft equipped with both chemical and solar electric propulsion, whose main goal is to safely capture the football size OS capsule and to bring it back to Earth. The Earth Return Orbiter (ERO) will be the biggest spacecraft ever to orbit Mars. The spacecraft will also be the first interplanetary spacecraft to rendezvous and capture a man-made object launched from another planet and return it to the Earth's surface, making a full round trip to Mars and back. ERO has also the secondary but essential mission to provide critical Mars-Earth communications coverage for Perseverance and the SRL. In addition, ERO will carry a radiation monitor that will measure the total radiation dose experienced by the spacecraft throughout the entire mission, which in addition to monitoring the health of ERO could provide important information on how to design systems for future human explorers. Launch is planned in 2027, entering into Mars orbit in 2029.

Figure 2. Earth Return Orbiter (ERO) with the Capture, Containment and Return System (CCRS) on its top. Credit: NASA/ESA/JPL-Caltech/GSFC/MSFC

ERO spacecraft hosts the NASA provided Capture, Containment and Return System (CCRS) which is tasked with capturing the OS, orienting it, sterilizing its exterior, and transferring it into a clean zone for secondary containment, toward safe return to Earth. To bring the OS into the CCRS, ERO will have in a first step to detect the OS, perform OS orbit determination and reach OS orbit. This leg is performed with ground in the loop. Once OS orbit is reached, ERO will start the rendezvous (RDV) leg, from typically 40km from the OS to capture. RDV relies on autonomous closed loop GNC using a vision system consisting in the NAC (Narrow Angle Camera) and the LiDAR (Light Detection And Ranging).
Present paper focuses on these two sensors and on the RDV leg.

1.3 The ERO vision sensors and image processing trade-off

The ERO vision system is firstly required to perform detection of the OS on its orbit around Mars with sufficient detection rate and accuracy to enable the OS orbit determination. The uncertainties on the OS insertion orbit imply to detect the OS at least once per synodic period and up to 1500km distance from ERO. Combined with the very small size of the OS (typically 20cm), this requirement is the most challenging for the vision system. The sensor trade-off, which also takes into account hardware mass, TRL and compactness constraints, has resulted in selecting a narrow angle camera (NAC) with a 4.5deg field of view (FoV) camera and a fainstar-2 sensor (1Mpx).

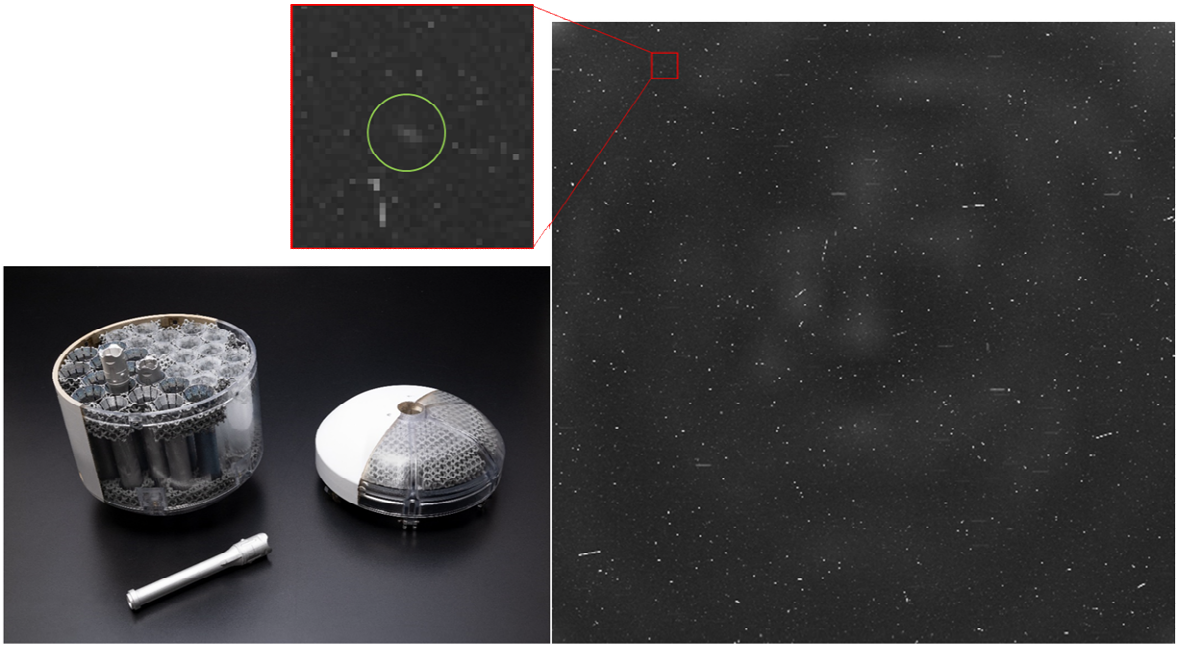

Figure 3. (Bottom left) Illustration of the OS (Credit: NASA/ESA/JPL-Caltech/GSFC/MSFC). (Right) Simulated image of the OS during OS detection phase (Upper left) Zoom on the OS (inside the green circle)

The second main requirement of the vision system is to provide real time OS position relative to ERO over the whole RDV leg. This legs starts at roughly 50km and ends with OS capture. It is divided into a far range part, where the vision system is asked to provide OS line of sight (LoS) only and not range, and a close range part where it shall provide LoS and range (or OS 3D relative position). For far range, NAC is directly used as OS detection requirements cover far range ones. To cope with real time closed loop need, a target centroiding (TgC) processing is integrated within the camera. Section 2 provides details on NAC and TgC.
For close range NAC does not respond to the need, as its images get blurry and saturated when approaching the OS (NAC is set to detect a very faint and far target, which implies a high

sensitivity and a high optical aperture). An additional vision unit is thus needed. Airbus considered 3 options: i) a monocular camera + model based image processing (see [3]), ii) stereo cameras with centroiding processing (see [4]), and iii) a LiDAR + 3D barycentring (see section 3.2). Table 1 summarises the pros and cons of each option.

Table 1: Trade-off on close range RDV vision system

	Mass	TRL	Complexity	Robustness
i) Monocular + mode based IP	++	-	--	--
ii) Stereo + centroiding	+	-	+	-
iii) LiDAR + 3D barycentring	-	+	+	++

Option i) has the main advantage over the others to have a low mass, as only one camera is needed, but suffers from medium TRL (TRL 7 for the camera and TRL 6 for IP) and high complexity. Option ii) is a good compromise between all criterions but lacks robustness to illumination conditions (Sun in FoV and eclipses). Option iii) has the drawback of mass, but offers high TRL (LiDARs are flying for several years to ISS) and high robustness to illumination conditions, enabling to provide GNC with measurements with very few outages. In addition, a LiDAR has the big advantage to intrinsically and directly measure the range, unlike cameras which measure LoS.
Despite its high mass, which relatively to ERO mass remains low, the LiDAR has finally been selected as the main RDV sensor for close range phase. It is described in section 3.

2 THE NARROW ANGLE CAMERA (NAC)

2.1 The sensor

The ERO NAC camera is based on existing HORUS (see [5] and [6]) star tracker, a new single-box star tracker available in 2021. Its development greatly benefits from the Navigation Camera experience, also designed by Sodern for the harsh environment of the JUICE Mission (see [7] and [8]).
The NAC is used for the OS detection phase in IMAGING mode (raw image acquisition to be processed on ground for OS orbit determination) and for the RDV phase in TARGET CENTROIDING (TgC) mode. For this latter mode, acquired images are directly processed by the camera to measure the OS line of sight (see §2.2).
The accommodation of the NAC opto-mechanical assembly is presented on Figure 4. The camera is designed in two main sub-assemblies (see [9]): the baffle, which-protects the camera from Straylight from Mars Limb and Sun, and the optical head, including a focal plane assembly based on the FaintStar2 CMOS detector, and a specific lens assembly.

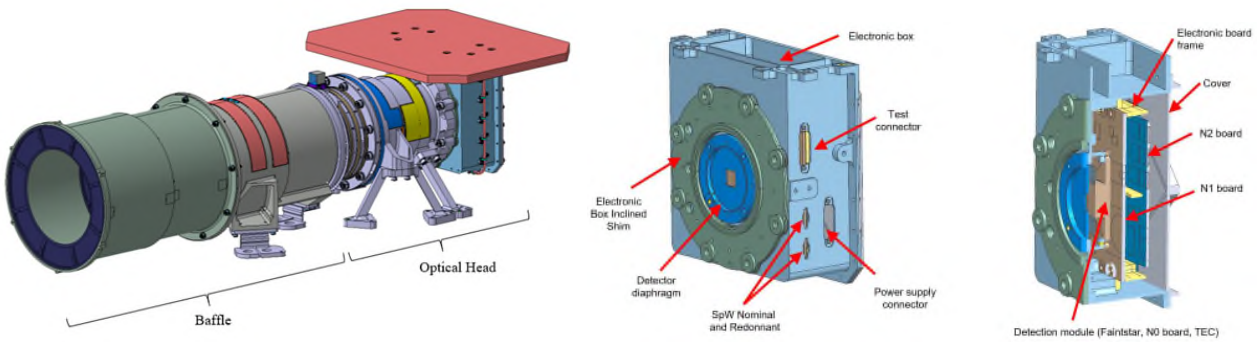

Figure 4. Narrow Angle Camera 3D (left) and its electronic box (right)

The baffle includes 5 black-coated vanes that form cavities and act as optical traps. A portion of the external surface of the baffle is coated with high-emissivity tape to evacuate heat. Due to its length (53cm), and for mechanical reasons, the baffle is a separate sub-assembly and is directly mounted on the NAC baseplate, using standoffs in an effort to minimize heat conductivity to the baseplate.
The optical head includes a dioptric lens assembly, which includes 11 lenses. Considering the ERO environment, the optical layout is based on radiation tolerant glasses, including some glasses developed specifically for Sodern and used in Star Tracker manufacturing. Moreover, the first lens is manufactured in fused silica for ionizing radiation shielding. A good control of the Point Spread Function (PSF) is necessary to ensure OS detection. For this reason, each individual lens is assembled in an optical mount, which position is adjusted during assembling operation.
The NAC Electronic box (see Figure 4) is based on the FaintStar2 monochrome, 1 Mega-pixel CMOS Image Sensor. The image sensor is assembled on a thermoelectric cooler (TEC) to ensure a sufficiently low temperature to minimize the impact of dark signal and defective pixels (hot pixels due to radiations) during the mission. The E-box includes three PCBs: one for the image sensor, one for FPGA, SDRAM and SpaceWire communication, and one for Power Supply of all NAC elements. In this standalone camera, the digital functions of the electronics allow to perform in parallel the image sensor sequencing and centroid computing as well as the thermal control of the detector and communication with ERO's on-board computer (OBC), using a single FPGA.

Table 2: NAC main features

Parameter	**Value**
Image Sensor	FaintStar2
Matrix size	1020x1020
Pixel encoding	12 bits
Camera field of view (circular)	4.5 deg
Lens focal length	129mm
Entrance pupil diameter	80mm
Baffle exclusion angle	14deg
Power supply	28V
Power consumption	<5W (standby), <12W (imaging, TgC)
Data interface	Redounded Spacewire link
Integration time (TgC mode)	458µs to 60s
Operating Sun phase angle (TgC mode)	0deg (Sun behind the camera) to 120deg

2.2 The image processing

During the RDV phase, NAC runs its internal image processing, the so called target centroiding (TgC), to provide in real time with frequencies between 0.1Hz and 0.5Hz the ERO GNC with OS centroid measurements. Main challenges of the TgC are to deal with the proton flux and the bright stars, which can lead to false alarms, and with the high dynamic range of the OS radiant flux (or magnitude). This latter reached a factor 10^6 between the minimum and the maximum OS fluxes (corresponds to 15 magnitudes), and is due to the high range of distances, from 70km to 400m, of Sun phase angles (from 0deg to 120deg), and to the OS "random" attitude caused by its tumbling motion (up to 30rpm).
The TgC has thus several filtering steps before computing the centroid:

1. Windowing, allowing for an optional reduction of the processing to a known or estimated region of interest, and for a reduction of undesirable bright pixels (stars, protons…)
2. Masking, of stars, defective pixels or other static perturbations identified during either ground or in-flight calibrations.
3. Thresholding, to derive a reduced family of pixels likely to contain the OS, using models

and look-up tables to predict its size and signal depending on mission parameters (distance, solar phase angle). This step is designed to be robust to OS random attitude (OS tumbling), background noise and straylight.

4. Filtering Protons, from this resulting family of pixels. This step makes use of the double image and rolling shutter sequencing of the Faintsar-2 detector to ensure consistency between lit pixels in both images originating from the selected family most likely to contain the OS.
5. Centroid and Quality Index computations, to ensure the detection of measurement outliers, and to provide insight to the OBC flight filter to quantify the likelihood of correctness of measurement.

3 THE LIDAR

3.1 The sensor

The RVS®3000 product family is the successor of Jena-Optronik's legacy RVS sensor, of which 48 units served flawless on flights to the International Space Station ISS on ATV, HTV and Cygnus spacecraft. The development of the RVS®3000 product family aims to enable a wide range of existing and potential future missions in guidance navigation applications, which require LIDAR-based measurement and analysis of 3D point clouds. So far, more than 10 RVS®3000 served in flights to ISS and 2 RVS®3000-3D (version with model-based pose estimation) were used by the mission-extension vehicles (MEV1 and MEV2) (see [10]) for docking to non-cooperative geostationary satellites.

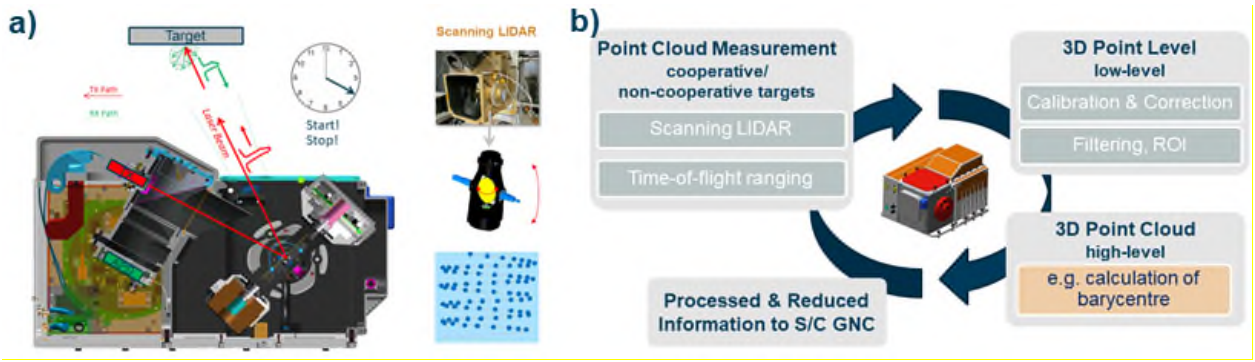

Figure 5. RVS3000 Product Family a) Scanning LIDAR based on time-of light measurement, b) Workflow of the RVS®3000 LIDAR product family for GNC applications

Space missions share a common workflow for a LIDAR in GNC see Figure 5 b). First, the LIDAR needs to acquire a 3D point cloud. To this end, The RVS®3000 makes use of scanning LIDAR technology and time-of-flight ranging. The combination allows flexible adaption of the point cloud angular resolution with virtually no dead pixel. Figure 5 b) recalls the concept for information. Next, low-level data processing results in a high-resolution precisely calibrated and corrected single shot accuracy. Afterwards, 3D processing capability of the RVS®3000 product family enable high-level analysis of the point cloud such as retro-reflector tracking, 6 degree-of-freedom pose estimation, or as in case of the MSR-ERO mission 3D calculation of the barycentre can be performed to extract the relevant information for the spacecraft GNC system. Further, several operational modes of the RVS®3000 enable a high level of autonomy. For example, the LIDAR acquire and track on its own with minimal need of GNC input or intervention. Thereby, ideally only processed and reduced information is shared with the GNC system.

3.2 The point cloud processing

Barycentre tracking is used for the MSR-ERO mission for ranges from 800m to the capture distance. The LIDAR acquires a 3D point cloud and calculates its 3D barycentre for each scan, at 0.5Hz for ranges higher than 100m, and 2Hz from 100m to capture. The field-of-view (FOV) centre and size adjusts autonomously from scan to scan based on a bounding box over the acquired point cloud. This enables the LIDAR to zoom in and out based on the visible features and to provide 3DOF information about the OS continuously.

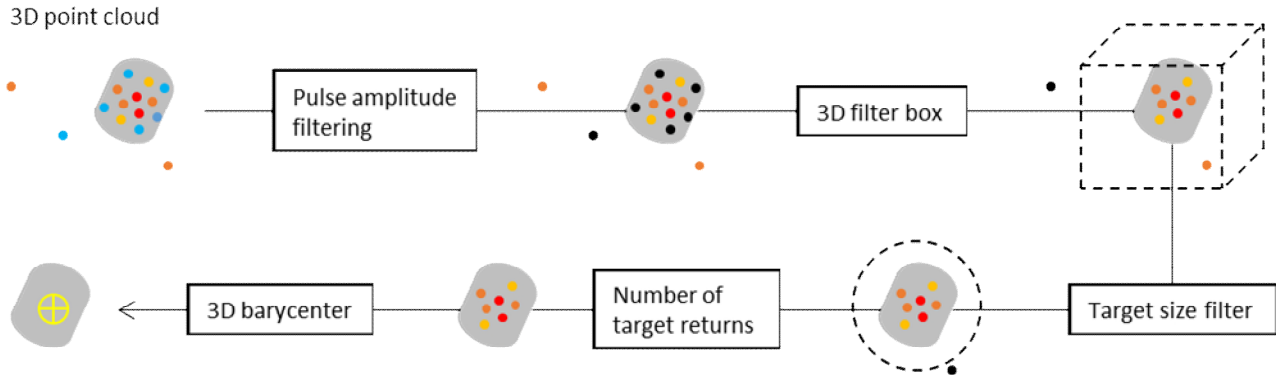

Figure 6. LiDAR point cloud processing steps

Figure 6 shows the principle of the LiDAR point cloud processing. Before computing the 3D barycentre of the target returns (TR) point cloud, several filters are applied to remove outliers. First TRs pulse with too low amplitude are discarded. Next, only TRs within a 3D box, which is defined from the previous scan are kept. Then, a priori known target radius is used to remove all TRs, which are too far away from the main point cloud. Finally, the number of remaining TRs is checked before 3D barycentre is computed.
The measured centre of geometry is in fact the barycentre of the target surface seen by the LiDAR. This results in an almost constant bias between the measurement and the real target centre of geometry. In the case of the OS, this bias is around 7cm and is taken into account by ERO's navigation function.

4 VISION SENSORS LAYOUT AND OPERATION

4.1 Layout

The NACs and LiDARs are mounted on the CCRS as close as possible to the CCRS's entrance to limit thermo-elastic biases between sensors measurement frames and CCRS's capture frame. LiDAR are tilted to enable OS measurements down to 1.2m (from this distance, ERO is not anymore controlled with vision in the loop).

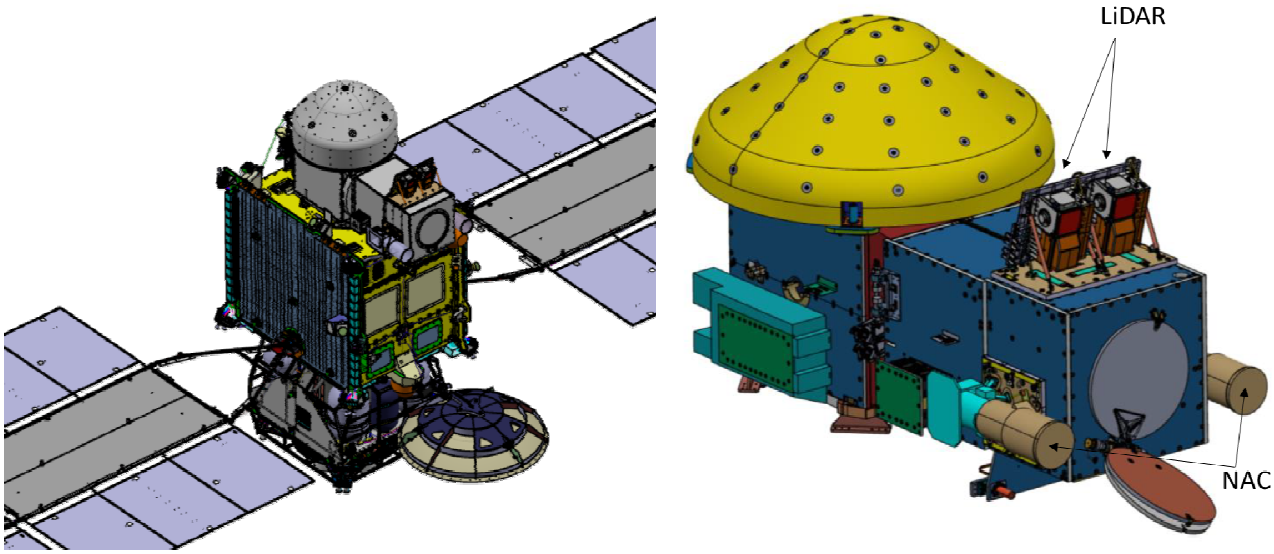

Figure 7. NAC and LiDAR layout on ERO

4.2 Far range leg

RDV starts when ERO has reached the OS orbit estimated by ground, at a distance to the OS of roughly 50km (see HIP in Figure 8). At this point, ERO has a very slow drift motion, due to OS orbit determination uncertainties, and will stay at HIP typically 24 hours.

NAC TgC is initialised during this time lapse. Several TgC computations are commanded on full frames images. The validity of the TgC output sequence is then evaluated by ERO's central software (CSW) by checking the consistency of the inter-frame motion of the targets detected by TgC with expected values. If NAC TgC sequence passes this validity check, TgC is then put in ERO's GNC closed loop and approach towards OS is started (S0).

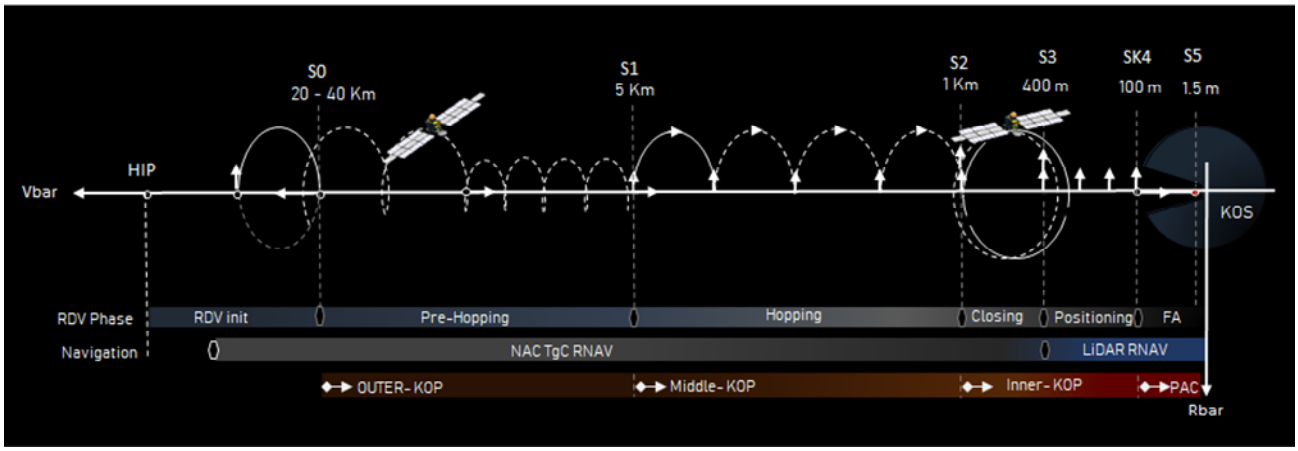

Figure 8. RDV trajectory

This approach consists in several tangential or radial boost manoeuvres bringing ERO to a pseudo station keeping oscillating between 1km (S2) and 400m (S3) distance to the OS. During this phase NAC TgC is commanded by CSW at 0.1Hz as long as the Sun illuminates the OS with a phase angle lower than 120deg. Out of this TgC operating domain, GNC works in pure navigation propagation. Within this domain, the CSW computes the appropriate NAC integration time and the TgC parameters (thresholds, star masks…) given on-board estimation of Sun phase angle and OS distance.

Both NACs (the nominal and the redundant) are commanded by the ERO's GNC to compute

centroids of the OS, but only the centroids measured by the nominal NAC are used by ERO's navigation function. On its part, the ground has the possibility to downlink images acquired by the NACs as well as their corresponding TgC outputs, to check the validity of these outputs.

4.3 NAC to LiDAR switch

Between S2 and S3 points (see Figure 8), first LiDAR measurements are acquired, whereas NAC continues to be used as main closed loop sensor. The CSW commands the LiDAR to find the OS in a 5°x5° window. Once the LiDAR has found the OS, it autonomously starts the tracking sequence and provides OS 3D position measurements to GNC at 0.5Hz. The measurements validity is checked by CSW (consistency with on-board navigation filter). Once validity is confirmed, LiDAR is put in ERO's GNC closed loop and ERO starts its close range approach.
Note that S2 distance is higher than LiDAR expected max range, so LiDAR is expected to lose tracking when getting close to S2 and needs CSW to reinitialise it afterwards.

4.4 Close range leg

After the LiDAR has replaced the NAC as main GNC sensor, the RDV close range leg begins. It is divided in two phases. The first consists in radial boost manoeuvres to reach a station keeping point (SK4, see Figure 8) at 100m from the OS. During this phase, both LiDARs are configured with the highest laser power level and with "long" scan duration of 2s. One LiDAR is used as nominal GNC sensor (its outputs are used by ERO's navigation function), and the other is used by GNC/FDIR for monitoring purpose (consistency check between both LiDARs).
Once SK4 is reached, both LiDARs are reconfigured to switch to their lower laser power level, and final forced translation is started. Both LiDARs are still used in hot redundancy (one for nominal GNC, one for monitoring) down to 1.2m. From this distance the OS partially goes out of LiDAR field of view and its measurements are not used anymore by GNC which finishes its trajectory in free drift until OS capture.
During both close range phases, the ground has the possibility to downlink LiDAR barycentring outputs and 3D point clouds for monitoring purpose and eventually to trigger a NO-GO toward GNC, which then will perform a retreat manoeuvre.

5 DEVELOPMENT PLAN AND PRELIMINARY PERFORMANCE

5.1 NAC development and validation

NAC follows a classical development process. Its preliminary design review (PDR) has been successfully held and its critical design review (CDR) is scheduled in Q3 2023. Several NAC mockups have been or will be manufactured by Sodern for testing purpose (shock, optical chain characterisation…). Three NAC units will be delivered by Sodern to Airbus: an engineering model (EM) in Q3 2023, a proto-flight model (PFM) and a flight model (FM) by end of 2024. NAC EM is used for functional and performance tests (straylight tests in particular), whereas electromagnetic compatibility (EMC), mechanical and thermal vacuum (TVAC) tests will be performed on PFM. PFM and FM will fly on ERO.

NAC performances for RDV are mainly assessed by image simulation. The image simulator is developed by Airbus and is based on Airbus in-house raytracer, the SurRender tool (see [11]). It integrates numerical models provided by Sodern to finely simulate all optical and electrical features of the NAC camera. These models have firstly been built from Sodern's past product experience and are being updated against dedicated measurement test campaigns performed by Sodern (PSF, straylight…).

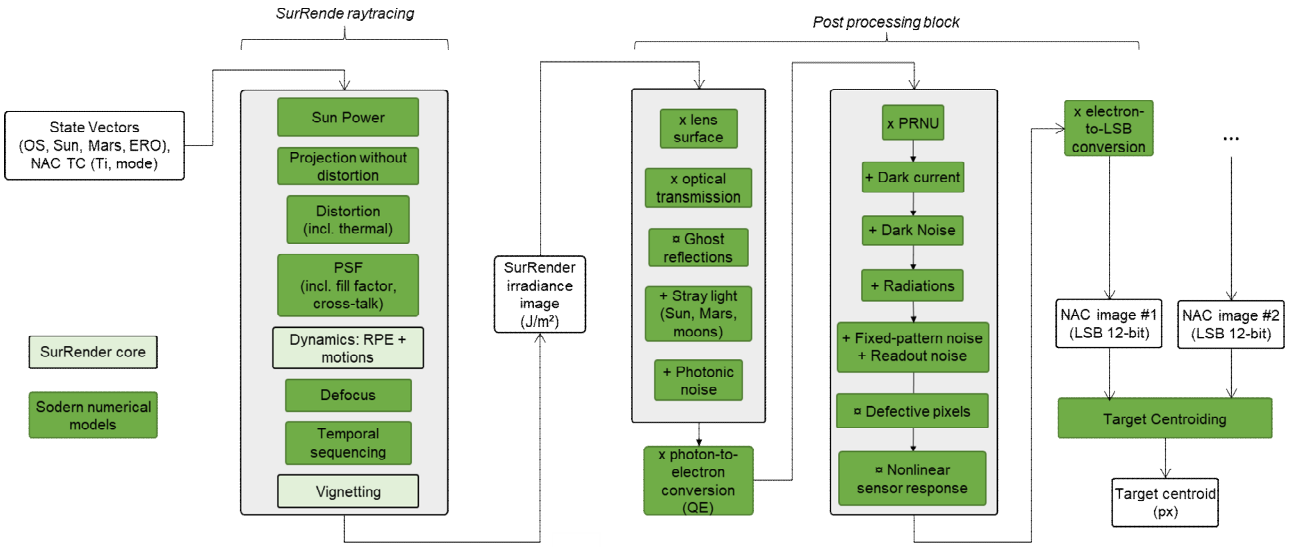

Figure 9. NAC image simulator diagram

The NAC image simulator covers all the mission phases where the NAC is used, from 1500km to 400m distance. Figure 3 shows an example of image simulated in the OS detection conditions. Proton impacts, star trails, straylight and noise can be easily observed. In Figure 10, two images simulated during RDV show a subpixellic (at 70km) and a resolved OS (at 400m). Note that background and noises are much lower during RDV than for OS detection phase, but still some protons and stars remain, which need to be filtered. Note also that at 400m, OS is saturating because minimum integration time of the detector is reached and is blurry because of NAC defocus (NAC focus is set to infinity).

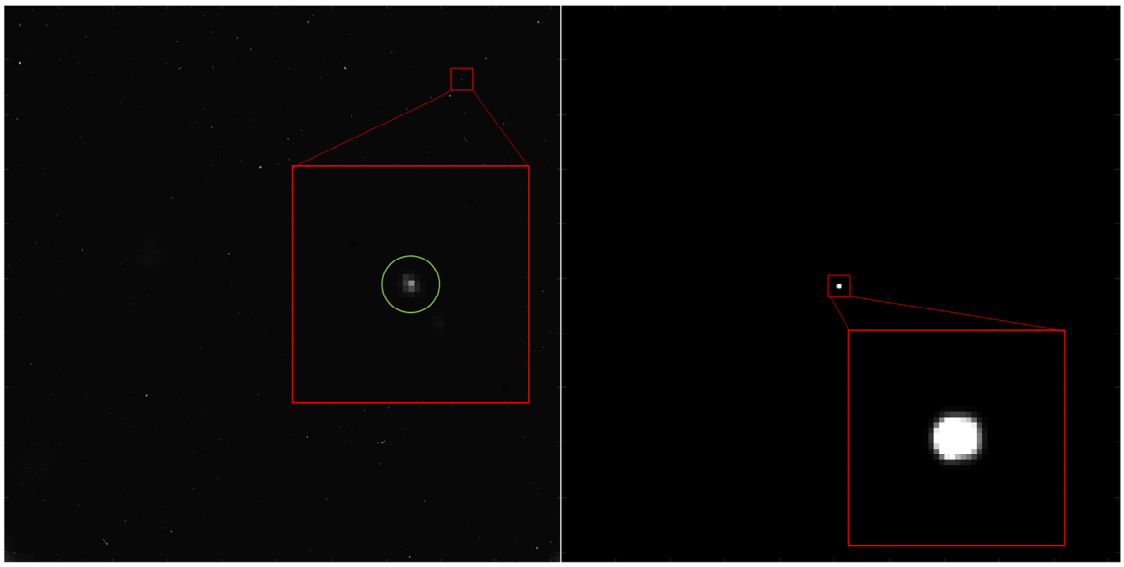

Figure 10. (Left) Simulated images of NAC at 70km with 120° Sun phase angle. (Right) at 400m with 60° Sun phase angle. (Red square) Zoom in on OS.

HW performance and functional validation of the NAC is performed in open loop by Sodern in its premises and during real sky test campaigns. During these campaigns real targets will be acquired from ground with the NAC EM. For OS detection, the NAC will be pointed to the sky by night toward satellites in Earth orbit and faint stars. For RDV phase, TgC will be tested by night on an OS mockup artificially illuminated to simulate the Sun.

A first simulation campaign has already been carried on to assess preliminary NAC TgC performances and check its compliance to specification. Table 3 shows the main TgC performances measured during this campaign.
A second simulation campaign, with complete and updated numerical models, and extensive amount of simulated images (~30 millions), will then be performed by end of 2023 to confirm and refine TgC preliminary performances.

Table 3: NAC TgC preliminary performances
(for OS distances from 400m to 70km and Sun phase angles from 0° to 120°)

LoS noise (1-sigma)	< 20µrad
LoS bias	< 20µrad
Valid measurement rate	> 95%
Outlier rate	< 0.1%

5.2 LiDAR development and validation

The MSR-ERO's LiDAR belongs to the family of the LIDAR developed for the ORION program, himself inherited from past JOP's LiDARs which fly for several years on various missions (see [12]). It therefore follows the review cycle dedicated to high TRL or COTS products. Its performance and functional validation strategy is however quite different from other projects, because of MSR-ERO mission specificities: a simple but small and tumbling target with no background, opposite to the large, cooperative and complex targets of missions for which JOP's LIDARs have been traditionally designed for.
Like for the NAC, a LiDAR EM will be delivered to Airbus in Q4 2023. LiDAR PFM, used for EMC and TVAC tests, and FM are expected beginning of 2025.

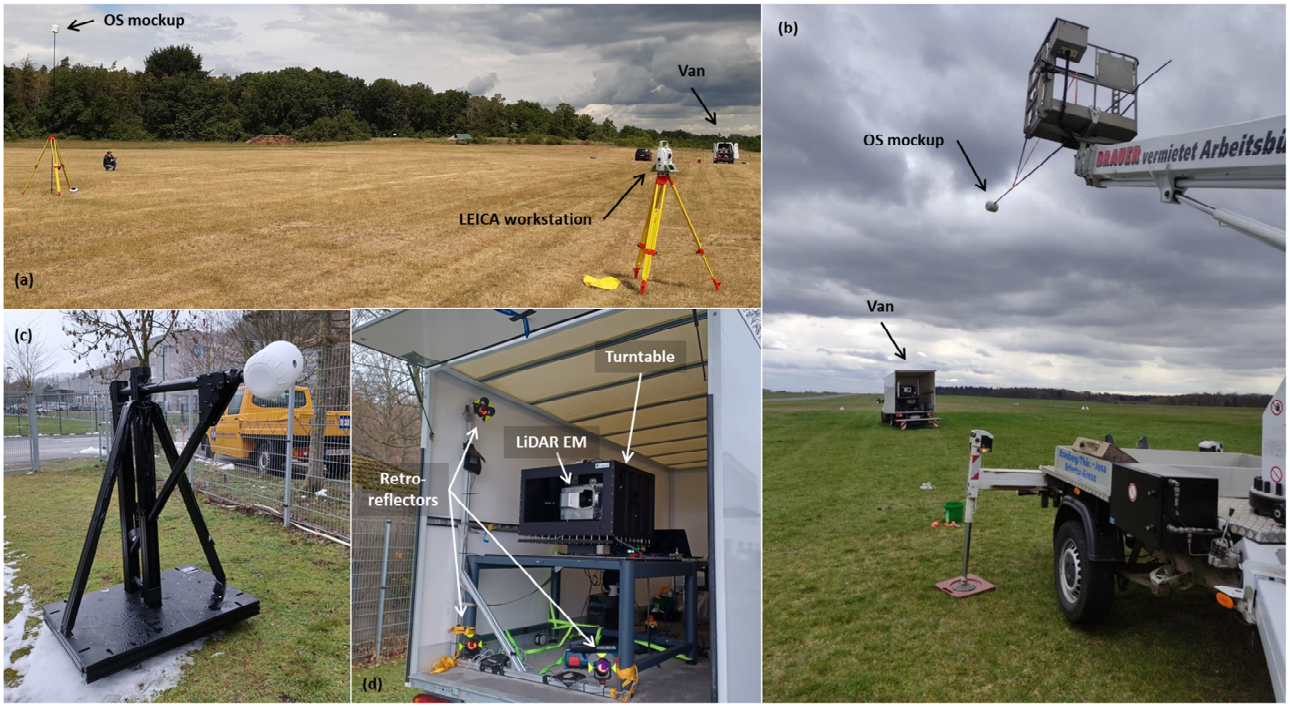

Figure 11. LiDAR tests on real target. (a) Ground truth is measured with a LEICA workstation. (b) LiDAR is mounted inside a van and OS is hanged to a crane. (c) OS is mounted on the tumbler. (d) LiDAR is placed inside a turntable. Retro-reflectors are located inside the van for ground truth.

However, unlike the NAC, the performance validation of the LiDAR in the MSR-ERO context

relies on tests on real target, rather than on simulation. JOP has developed several test means adapted to MSR-ERO, like a turntable to simulate ERO's pointing stability or a tumbler to simulate OS tumbling in free space (see Figure 11). Test are performed outdoor to cope with real and long distances for which LiDAR is expected to work (scaled tests are not possible with a LiDAR, unlike a camera). The ground truth, against which LiDAR measurements are compared for performance assessment, is obtained with a LEICA workstation. The latter, which is much more accurate than the JOP's LiDAR (but much slower!), measures the LiDAR position, thanks to retro reflectors located around the LiDAR, as well as the OS position, directly by scanning the OS.

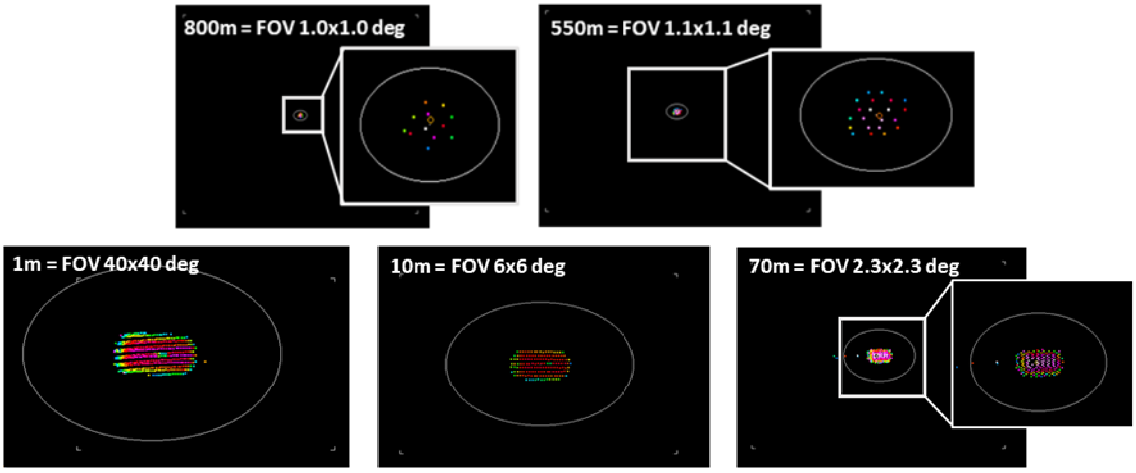

Figure 12. Example of the measured point clouds including barycentre for various distances and LIDAR FOV settings.

Three test campaigns have already been performed and enabled to collect several test data. Their analysis gives the OS position error as function of range from ranges between 1 m and 800 m. At close range, many laser shots are distributed over the OS mock-up despite a large LIDAR FOV. Narrowing the LIDAR FOV with increased distance allows to achieve sufficient point density on the target. Robust performance is indicated to very long ranges to around 800 m, as still several range measurements with sufficient return amplitude from the OS mock-up are available for barycentre calculation (see Figure 12). LiDAR preliminary performances assessed from test campaigns are presented in Table 4.

Table 4: LiDAR preliminary performances
(d_{OS} = OS distance)

	d_{OS} < 100m	**100m < d_{OS} < 800 m**
LoS noise (1-sigma)	0.06 deg	0.015 deg
LoS bias (max)	0.15 deg	0.15 deg
Range noise (1-sigma)	0.01 m	0.02 m
Range bias (max)	0.1 m	0.25 m

A final LiDAR test campaign is foreseen in summer 2023 to verify, before LiDAR EM delivery, the LiDAR performances, its tuning for MSR-ERO, and the good functional behaviour of LiDAR in MSR-ERO conditions.

5.3 Integration into the GNC development plan

MSR-ERO NAC and LiDAR are validated in open loop by Sodern and JOP in their premises (see sections 5.1 and 5.2). Their integration within the ERO's avionic and their functional validation is

then done by Airbus in two steps: by simulation, using the GNC FAME simulator and with HW in the loop using the avionics test bench (AVM).
The FAME simulator aims at designing and validating the overall ERO's GNC over all MSR-ERO mission phases (including RDV). In the simulator, NAC and LiDAR are modelled through core functional models (CFM), which are numerical model of the sensors. A CFM models both the sensor interfaces (TM/TC) and the sensor performances of its overall measurement chain (optical chain + data processing). In simplified terms, the CFM performance bloc takes as input the perfect position of the OS and add covering and representative sensor errors to it. NAC and LiDAR CFM are designed and tuned jointly by Sodern, JOP and Airbus, using tests data acquired or simulated during NAC and LiDAR test campaigns performed by both suppliers.

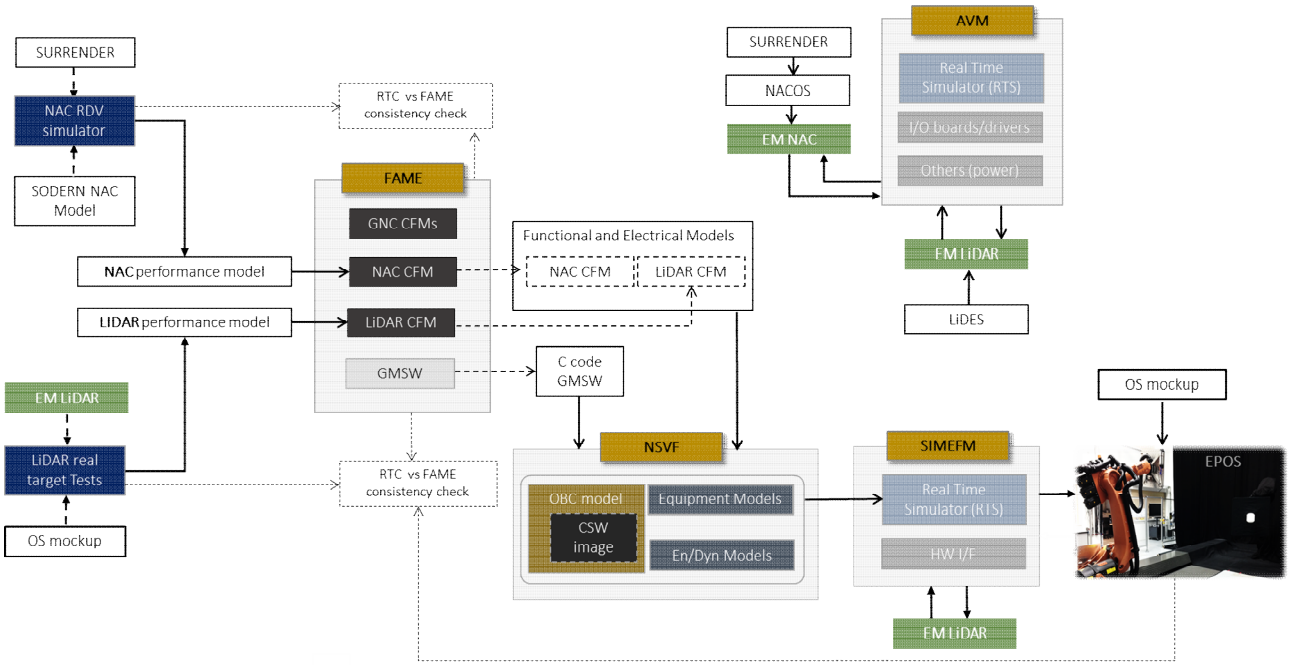

Figure 13. NAC and LiDAR within the RDV GNC validation strategy (SurRender is the inhouse raytracer tool, FAME is the ADS's GNC simulator, AVM is the "flatsat" test bench, GMSW is the GNC SW, NACOS is the NAC optical stimulator and LiDES is the LiDAR electrical stimulator)

After reception of the sensor EMs, the second step of functional validation begins. It consists in HW in the loop tests. NAC and LiDAR EMs are integrated in the AVM test bench (equivalent to a flat sat) and stimulated by dedicated means. The NAC is stimulated by an optical stimulator, called the NACOS (NAC Optical Stimulator), built by Airbus and derived from star tracker stimulator and JUICE NavCam stimulator (see [13]). The NACOS will mainly be used for RDV far leg phase when NAC is used in closed loop. For its part, the LiDAR will be stimulated electronically by a stimulator provided by JOP which simulates point cloud and write them directly onto the LiDAR's memory, before being processed by the LiDAR. Both simulators run in real time, use an OS CAD model with appropriate optical properties and simulate MSR-ERO environment and dynamics.

Finally, as an ultimate test to validate RDV GNC with HW in the loop, GNC SW will be tested at the EPOS robotic test facility (ref). The test will include the LiDAR EM, the GNC SW implemented on an emulated OBC, and an OS mockup. Due to EPOS facility constraints and the impossibility to scale LiDAR's tests, only the last meters before capture will be simulated.

6 CONCLUSION

The rendezvous (RDV) leg of MSR-ERO mission relies on two GNC sensors: the NAC (narrow angle camera) built by Sodern and used during far range RDV, and the LiDAR provided by JOP and used during close range part. Both sensors have successfully passed ERO's system PDR (preliminary design review) and are on the way for the upcoming CDR (critical design review).
Preliminary open loop performance campaigns have been performed by simulation for NAC and by test for LiDAR. They have confirmed the compliance of both sensors to GNC requirements, keeping ESA and Airbus confident in their suitability to enable a safe and precise capture of the (OS) by ERO.
Engineering models of both sensors are currently being manufactured and will be delivered to Airbus by end of 2023, paving the way to their integration in ERO's spacecraft, before the deliveries of the flight models in 2024/2025.

7 REFERENCES

[1] Muirhead B. K., Nicholas A. K., Umland J., Sutherland O., Vijendran S., *Mars Sample Return Campaign Concept Status*, Acta Astronautica, Vol. 176, 131 – 138, 2020.

[2] Simon J. I., et al., *Samples Collected from the Floor of Jezero Crater with the Mars 2020 Perseverance Rover*, Journal of Geophysical Research: Planets, Vol. 128, e2022JE007474. https://doi.org/10.1029/2022JE007474.

[3] Burri M., et al., *Mars Sample Return - Test Campaign for Near Range Image Processing on European Proximity Operations Simulator*, 11th International ESA Conference on Guidance, Navigation & Control Systems, 2021.

[4] Segal S., Carmi A., Gurfil P., *Stereovision-based estimation of relative dynamics between non cooperative satellites: Theory and experiments*. IEEE Trans. Control. Syst. Technol. 2014, 22, 568–584.

[5] Fullenbaum F., et. al., *Horus: A star tracker for space super highways*, AAS23-xxx (submitted), 2023

[6] Gelin B., et. al., *Horus star tracker*, AAS23-134 (submitted), 2023

[7] Nicollet L., et. al., *Design of a vision-based navigation camera for juice*, GNC ESA 17, 2017.

[8] Gorog F., et. al., *Juice navigation camera design*, ESA GNC 21, 2021.

[9] Goux P., et. al., *MSR-ERO : Narrow Angle Navigation Camera*, GNC ESA 23, 12, submitted

[10] Pyrak M., Anderson J., *Performance of Northrop Grumman's Mission Extension Vehicle (MEV) RPO Imagers at GEO*, Advanced Maui Optical and Space Surveillance Technologies Conference (AMOS). 2021

[11] Lebreton J., Brochard R., et al., *Image Simulation for space applications with the SurRender*

software. 2021. 11th International ESA Conference on Guidance, Navigation & Control Systems. https://arxiv.org/abs/2106.11322

[12] https://www.jena-optronik.de/products/rendezvous-sensors/applications.html

[13] Jonniaux G., Regnier, et al., *Development, tests and results of onboard image processing for JUICE*, Proceedings of the 9th International ESA conference on Guidance, Navigation and Control Systems. 2021